Control of morphology and nanostructure of copper and cobalt oxalates: Effect of complexing ions, polymeric additives and molecular weight†

Paul Bowen,* Ollivier Pujol, Nathalie Jongen, Jacques Lemaître, Alke Fink, Pierre Stadleman and Heinrich Hofmann

Received 18th June 2010, Accepted 1st September 2010
DOI: 10.1039/c0nr00420k

Precipitated oxalates are often nanostructured and can be used as precursors for nanostructured oxides for different applications. The modification of the particle shape and nanostructures of both copper and cobalt oxalates has been demonstrated using polymeric additives or complexing counter-ions. In the case of cobalt oxalate the characteristic elongated rod particle shape (axial ratio of 10) can be modified by using polymethymethacrylate (PMMA) to produce particles with lower axial ratios of 2, through cubes all the way to platelets (axial ratio 0.2). The PMMA inhibits the growth of the particles along the [101] direction more and more strongly as the concentration of the polymer increases. The crystallite size from XRD line broadening is not modified by the PMMA indicating that the PMMA does not influence the nucleation and growth but modifies the aggregation kinetics. Copper oxalates precipitated in the presence of different cellulose derived polymers with different molecular weights and functional groups (methyl and propyl) showed sensitivity to both molecular weight and functional group. Higher molecular weights did not influence the copper oxalate particle shape, whereas methyl cellulose gave elongated particles and propyl celluloses gave platelet like particles. Copper oxalate precipitated in the presence of acetate counter ions gave platelets with an axial ratio of 0.15 compared to the cushion-like morphology (axial ratio 0.5). The primary crystallites were more elongated along the [001] direction in the presence of acetate, modifying the proportion of the hydrophobic and hydrophilic surfaces and hence influencing the aggregation kinetics and particle shape. The copper and cobalt oxalate particle formation seems to be dominated by the primary particle aggregation with the different additives interacting specifically with different crystallographic faces of the primary particles. By tuning this interaction particles with different shapes and substructures can be formed.

Introduction

Many commercial products are formulated from precipitated particles using either organic or inorganic chemicals. It is desirable to control the properties of the precipitate with respect to its chemical composition, its size, its substructure and its shape. The control of the particle structure at the nanoscale may provide new particles with specific hierarchies for specific applications with optimum properties as often seen in nature.[1–4] Additives, such as polymeric molecules, are often used to modify the particle shapes and substructures but the mechanisms behind their action are not always well understood. A better understanding both at a qualitative level and molecular level are needed to provide us with the tools to control better the production of nanostructured particles. In the current paper two systems which produce nanostructured particles by self-assembly, copper oxalate[5] and cobalt oxalate[6] are studied in more detail. The role of a series of polymeric additives and complexing counter-ions are investigated to try and provide a better understanding and control of the nanostructured particle formation.

Precipitated oxalates often have nanosized crystallites and the aggregation or self assembly of these primary crystallites can be influenced by reaction conditions or by the use of additives.[5–7] The oxalates are often precursors for oxides and the oxides can retain the nanostructure, particle shape and crystallite arrangement after thermal decomposition.[8,9] The resulting oxides can be used as in various catalytic applications *e.g.* such as copper oxide for water purification.[10] There are many examples of the effect of additives on the growth and self-assembly of nanostructured precipitates.[11–14] For copper oxalate without additives, particles with a cushion-like morphology are observed while increasing the concentration of hydroxypropylmethylcellulose (HPMC) induces a variation of the shape from low axial ratio cubes to higher axial ratio rods.[5] The crystallites within these particles showed a more elongated shape and smaller size as the HPMC concentration was increased. The polymer additive influenced the 3 steps of copper oxalate precipitation: nucleation, crystal growth and aggregation. The way the copper oxalate crystal unit cell is defined seems to induce two types of crystallite surfaces, one more hydrophilic and one more hydrophobic.[5] The first type denoted α is perpendicular to the [001] direction and are expected to have polar terminations. The second type denoted ε is perpendicular to either the [110] or [1$\bar{1}$0] directions. The ε faces should not contain any free bonds in the oxalate groups that

Powder Technology Laboratory, Materials Science and Engineering Department, EPFL, CH-1015 Lausanne, Switzerland. E-mail: paul.bowen@epfl.ch

† Electronic supplementary information (ESI) available: Solubility calculations; distribution of dissolved Cu species; Tables S1–4; X-ray powder diffraction data; cobalt oxalate crystallographic monoclinic structure; thermogravimetric analysis. See DOI: 10.1039/c0nr00420k

terminate at the surface, thus it is expected to be of low polarity and consequently relatively hydrophobic—the interaction of the HPMC with these different surfaces consequently determined the growth and self-assembly mechanism, generally termed brick-by-brick.[1]

To try to understand better the role of the HPMC and how the different functional groups and molecular weights may influence the interaction of the polymer with the copper oxalate growth, a series of cellulose derivatives with different functional groups but similar molecular weights and the same functional groups and different molecular weights have been investigated. In addition to the effect of additives, Matijevic has often shown the particularly significant influence of counter-ions on the particle morphology.[15,16] In the present study, we modify the copper oxalate precipitation conditions by adding a copper complexing agent in the form of acetate ions. The effect of the dissolved species concentrations on the primary crystallite size, copper oxalate structure and particle morphology is demonstrated and discussed using speciation calculations from a thermodynamic model.[17] Cobalt oxalate has also been demonstrated to be a nanostructured oxalate with a complex core–shell structure—producing elongated acicular particles.[6] The influence of a polymeric additive (polymethylmethcarylate PMMA) on its growth and particle morphology has been investigated and shows significant influences on the particle morphology. By using a series of characterization techniques the influence of PMMA on the growth mechanism is deduced.

Experimental

Precipitation was carried out by simultaneously adding a copper or cobalt nitrate solution (250 mL h^{-1}) and a sodium oxalate solution (250 mL h^{-1}) to a saturated copper or cobalt oxalate solution (100 to 500 mL) in a 2 L stirred batch reactor maintained at 30 °C in a water bath. The copper mother solution contained 2.22×10^{-4} mol L^{-1} of copper nitrate, and sodium oxalate and 1.1×10^{-5} mol L^{-1} of nitric acid (pH around 5) with varying types of polymeric additives (see Table 1, all at 0.0195 g L^{-1}). The cobalt mother solution contained 5.1×10^{-5} mol L^{-1} of cobalt nitrate and sodium oxalate with varying concentrations of nitric acid (to keep the pH around 6) and polymethylmethacrylate (PMMA) at 7 different concentrations (2.5, 12.5, 16.7, 20, 50, 200 and 800 mg L^{-1}) (Table 1) The composition of the reactant solutions was 4×10^{-2} mol L^{-1} of copper nitrate and sodium oxalate and 3.989×10^{-2} mol L^{-1} cobalt nitrate and 4.07×10^{-2} mol L^{-1} sodium oxalate. After adding the reactants, the suspension was aged under agitation for 30 min (cobalt) or 60 min (copper). The copper precipitates were allowed to sediment (1 h) and then centrifuged to remove the filtrate. The cobalt was allowed to settle for 30 min. Precipitates were then filtered on a 0.2 μm membrane and dried over silica gel in a desiccator until a constant weight was obtained.

Table 1 Types and characteristics of the different polymeric additives used in the precipitation of cobalt and copper oxalates

	Polymer	M_n/g mol^{-1}	M_w/g mol^{-1}	M_w/M_n
PMMA	Polymethylmethycrylate	3250	4030	1.14
HPMC 50	Hydroxypropylmethyl cellulose	33 700	155 000	4.60
HPMC 100	Hydroxypropylmethyl cellulose	38 000	205 000	5.38
HPMC 400	Hydroxypropylmethyl cellulose	64 000	351 000	5.45
MC 25	Methyl cellulose	21 000	94 000	4.44
HPC EF	Hyroxypropyl cellulose	21 000	77 000	3.66
HPC MF	Hydroxypropyl cellulose	19 000	280 000	14.9

A series of experiments were carried out where copper acetate was added to the copper nitrate solution. The copper solution was composed of 2×10^{-2} mol L^{-1} of copper nitrate and 2×10^{-2} mol L^{-1} of copper acetate and simultaneously mixed with 4×10^{-2} mol L^{-1} of sodium oxalate. The mother solution contained 3.12×10^{-4} mol L^{-1} of copper acetate, 3.12×10^{-4} mol L^{-1} of sodium oxalate and 2×10^{-2} mol L^{-1} of sodium acetate.

The precipitated powders were observed in scanning electron microscopy (SEM Jeol JSM-6300F, Philips YL30-SFEG) and Transmission electron microscopy ((Philips EM-430-T) operating at 300 kV and −184 °C. X-Ray powder diffraction (XRD) was carried out using a Siemens D500 diffractometer and mean crystallite size from the peak broadening using either the Scherrer equation[18] or Warren–Averbach method[19] depending on the number of reflections for the different crystallographic dimensions.[5,6] Thermogravimetric analysis was performed under flowing air (200 mL h^{-1}) (copper) or nitrogen (cobalt) using a Mettler TA4000 thermobalance. The samples were measured from 30 °C to 405 °C (cobalt) or 900 °C (copper) with a heating rate of 10 °C min^{-1}. Some samples were analysed using Fourier transform infrared spectroscopy (FTIR) in the attenuated total reflectance mode (Perkin Elmer Spectrum BX).

Solubility calculations of copper oxalate in the presence of acetate ions in the system $Cu(OH)_2$–$H_2C_2O_4$–HAc–[HNO_3/NaOH]–H_2O were carried out and the details of the method and the effect of this complexing agent on the distribution of dissolved species are presented in the ESI (S1).†

Results and discussion

Effect of polymethylmethacrylate (PMMA) on cobalt oxalate precipitation

For all PMMA concentrations, 2.5 to 800 mg L^{-1}, the precipitated phase was cobalt oxalate di-hydrate (COD) $CoC_2O_4 \cdot 2H_20$, indexed with a monoclinic structure[5,20] with no effect of the PMMA on the unit cell (see the ESI (S2)†). The effect on the morphology was however significant at PMMA concentrations above 2.5 mg L^{-1} as can be seen in Fig. 1 where the particles change from their expected acicular rod shape[6] at 2.5 mg L^{-1} to cubes at 16.7 mg L^{-1} and finally to platelets at PMMA concentrations above 200 mg L^{-1}. The crystallographic orientation of the crystallites in the acicular particles (2.5 mg L^{-1} PMMA) has been shown previously to follow the [101] direction and that the rods are built up by a brick-by-brick mechanism by oriented attachment along this crystallographic direction.[1,6] Thus, at first view it seems that the PMMA interferes with this growth and inhibits growth more and more strongly along this [101] direction without greatly effecting the (−101) and (010) faces that make up the sides of the rods. Thus as we increase the PMMA

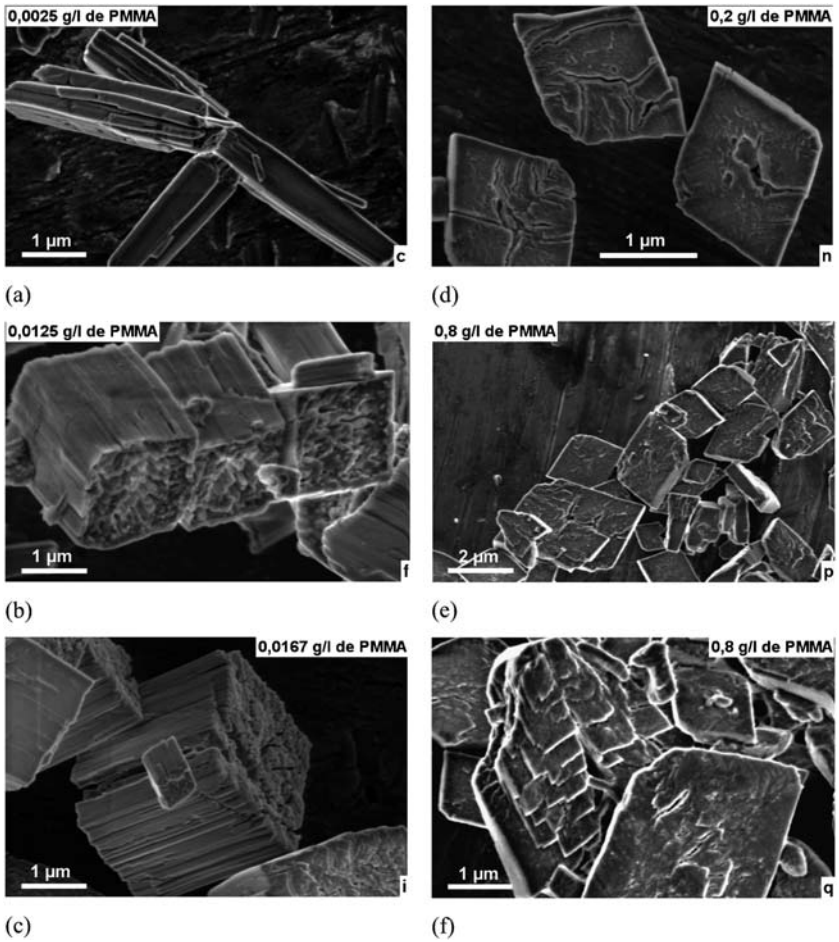

Fig. 1 HSREM images of cobalt oxalate precipitates in the presence of different concentrations of PMMA in mg L^{-1}(a) 2.5, (b) 12.5, (c) 16.7, (d) 200, (e) 800, (f) 800.

concentration the (101) faces of the particle go from having the smallest relative area (end of rods) to the largest relative area (faces of platelets).

To verify that the platelet faces are in fact the (101) faces, electron diffraction was carried out in the TEM. Fig. 2a shows a TEM image of a COD particle precipitated in the presence of 800 mg L^{-1} PMMA. Fig. 2b shows the electron diffraction pattern indexed corresponding to the [101] zone axis. The pattern is characteristic of a defective single crystal (presence of twins)

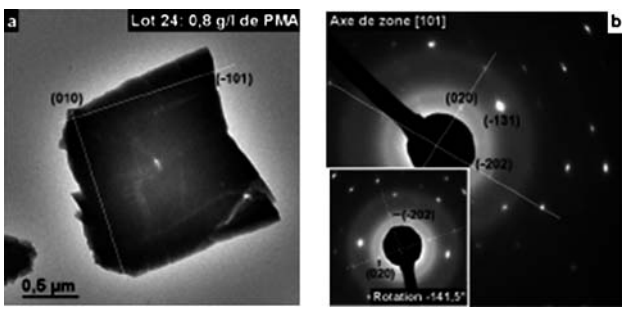

Fig. 2 (a) TEM image of cobalt oxalate preciptate (800 mg L^{-1} PMMA) showing a platelet with indexation of the faces; (b) electron diffraction pattern indexed along zone axis [101] of the platelet imaged in (a).

superimposed on an amorphous phase (diffuse rings) coherent with the core–shell structure found for the acicular particles previously.[6] The diffraction pattern allowed us to confirm that the face normal to the electron beam is the (101) face with the platelet edges corresponding to the (−101) and (101) faces as marked in Fig. 2a.

The (101) faces are perpendicular to the cobalt oxalate molecular units that form "ribbons" in the crystal structure (see ESI, S3†) and these faces may terminate with an oxalate group. The carboxylate group of the PMMA molecules would be expected to compete for the cobalt terminating this face with an oxalate carboxylate group, as polyacrylates are known to form complexes with bivalent ions.[21–24] This would significantly reduce growth along this direction. The adsorption of PMMA could not be detected in the TGA data as the decomposition of the PMMA and the decomposition of the cobalt oxalate overlap at around 400 °C (see ESI, S4†). However by FTIR a characteristic vibrational mode of a C–O elongation for PMMA at around 1100 to 1220 cm, where COD does not have any characteristic modes, could be resolved (Fig. 3a). Fig. 3b shows that the presence of PMMA increases with increasing PMMA content in the reaction mixture. When observing the particles in the HRSEM, the different particles faces behaved quite differently. The (010) and (−101) faces were stable under the electron beam whereas

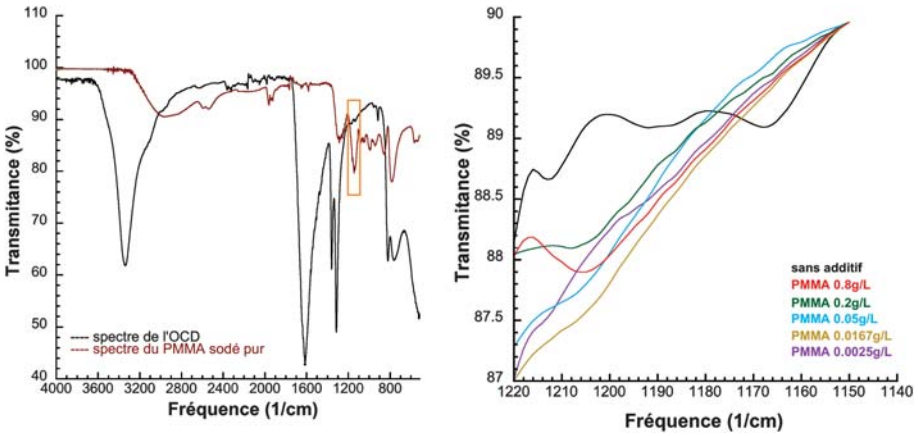

Fig. 3 FTIR spectra for (a) cobalt oxalate dehydrate (OCD) and PMMA (b) precipitated cobalt oxalates with different concentrations of PMMA showing the presence of PMMA in the range 1190 to 1220 (cm^{-1}).

the (101) faces became more and more sensitive to the electron beam as the PMMA concentration increased. The cracks on the faces of the particles in Fig. 1 (d), (e), (f) were induced by the electron beam. This again supports the idea that the PMMA specifically adsorbs onto these (101) faces and with a higher amount as the PMMA concentration increases.

XRD crystallite sizes were calculated from line broadening[18] and results for 3 precipitates are shown in Table 2. The results show that the crystallite sizes are very similar for the precipitates without and with additives indicate that the PMMA does not influence the crystallite size despite the significant change in morphology. Also the yield of precipitated powder was around 90% of that predicted theoretically, indicating that the amount of powder collected with and without the PMMA was constant. That there is no influence on the size or number of crystallites, indicates that the PMMA does not influence the nucleation and growth of the crystallites but acts on the self-assembly and aggregation process. This suggests that aggregation *via* the (101) faces is significantly less favourable because of a preferential adsorption of the PMMA on this face as postulated above. As the PMMA concentration increases, the coverage and residence time of the PMMA on the 101 faces should increase and thus hinder the aggregation in this direction, giving us the development of particles with axial ratios below 1. From the TEM images the axial ratio of the particles were calculated (from about 20 particles) and the change in morphology as a function of PMMA is illustrated in Fig. 4. The modification of the aggregation kinetics by specific adsorption onto different crystallographic faces has also been recently demonstrated for copper oxalate in the presence of glycerin.[7]

Table 2 Crystallite sizes for precipitated cobalt oxalate di-hydrates without additive and in the presence of PMMA at 2 concentrations

Powder	Crystallite size/nm[a]	Direction
Without additive	27	[−111]
	10	[202]
	31	[111]
	10	[040]
0.025 g L^{-1} PMMA	24	[−111]
	9	[202]
	33	[111]
	8.5	[040]
0–8 g L^{-1} PMMA	24	[−111]
	9	[202]
	29	[111]
	10.5	[040]

[a] Error around ±1 nm.

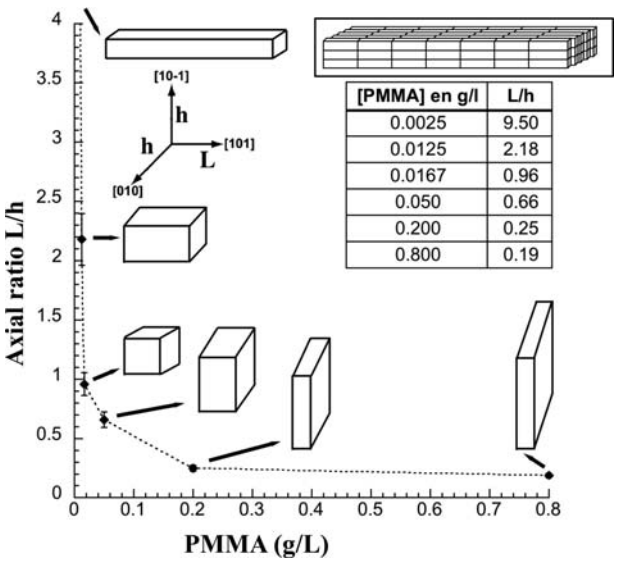

Fig. 4 Control of axial ratio for precipitated cobalt oxalate dehydrate (COD) in the presence of different concentrations of PMMA—measured from TEM images. The inset schematically illustrates that all the particles are composed of iso-oriented nanocrystals.

Nanostructured copper oxalate effect of modified cellulose derivatives of different functional groups and molecular weight

The influence of HPMC on the growth morphology of copper oxalate was in fact discovered by accident as we tried to coat the Teflon tube of a tubular reactor to avoid fouling of the reactor walls.[25] We then made a systematic study of the HPMC varying its concentration which allowed control of crystallite and particle size.[5] To try and further elucidate how the HPMC interacts with

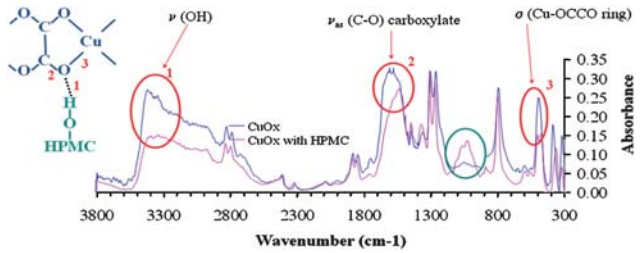

Fig. 5 FTIR spectra for copper oxalate precipitates with and without the presence of HPMC indicating some degree of hydrogen bonding between the HPMC and copper oxalate.

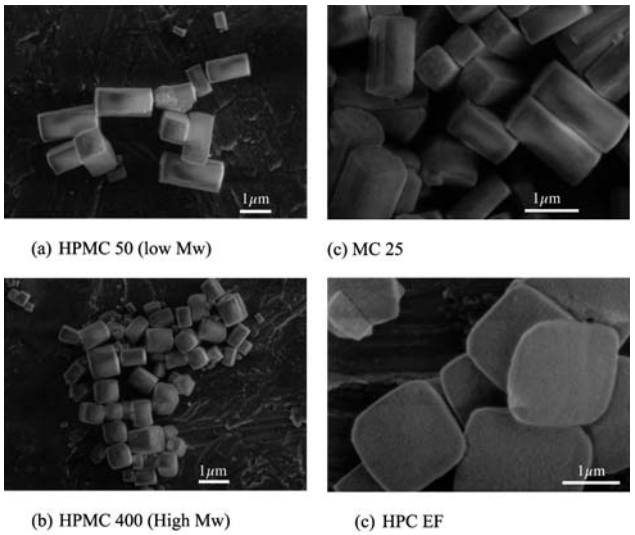

Fig. 6 SEM micrographs showing morphological changes of copper oxlate precipitates (a) and (b) HPMCs of different molecular weights (M_w) and different functional groups: (c) methyl cellulose; (d) propyl cellulose.

the copper oxalate surface we carried out FTIR analysis of the copper oxalate with and without HPMC. The FTIR showed modification in the water and hydroxyl absorption profiles around 3400 cm^{-1}, in the asymmetric carboxylate band at 1700 cm^{-1} and the Cu–OCCO bands at 500 cm^{-1}. As well as these modifications a new absorption band between 900 and 1100 cm^{-1} was interpreted as being indicative of hydrogen bonding between a hydroxyl group of the HPMC and oxygen in the oxalate ribbon (Fig. 5).

To try and further clarify the role of the functional groups, the influence of a series of polymeric cellulose derivatives on the copper oxalate precipitated morphology were carried out. Different molecular weights and different degrees of substitution of the methyl and propyl groups, as well as a hydroxyethylcellulose (HEC) were investigated. The molecular weights and degree of substitution are given in Table 1. All experiments were carried out with the same concentration of polymer (0.0195 g L^{-1}) which with the original HPMC 100 used in previous studies gave square ended rods,[5] an intermediate morphology between the cushions found without additives and the high aspect ratio rods with higher concentrations (>0.1 g L^{-1}). For HPMC, 3 molecular weights were investigated and all had similar degrees of methyl and propyl substitution of around 26% and 4% respectively. The effect on morphology can be seen in Fig. 6, where the lower molecular weight HPMC 50 gives a similar square ended rod morphology to HPMC 100 (Fig. 6 (a)), whereas the higher molecular weight HPMC 400 was less effective, with cubic particles being formed (Fig. 6(b)). When a polymer containing only methyl substitutions (MC25) with a similar molecular weight to HPMC 100 was used, similar morphologies were obtained (Fig. 6(c)). For two hydroxyproyl substituted polymers, the same trend in molecular weight was seen the higher M_w cellulose HPC MF, which showed no influence on morphology giving cushions; while the lower M_w HPC EF gave platelets (Fig. 6(d)). These results suggest that when the molecular weight is too high the inhibition of growth by aggregation is less efficient, this has also been seen in the synthesis of nanostructured calcite in the presence of polyacrylic acid PAA.[26] In the case of calcite this has been interpreted as a kinetic effect where the larger molecules do not adsorb quickly enough to influence the relatively rapid aggregation kinetics. Attempts to quantify the adsorption kinetics *versus* the aggregation kinetics have so far been unsuccessful in the copper oxalate system—even using synchrotron radiation at ELLETRA—either the copper concentration is too low for particle detection or the kinetics of aggregation become too rapid (<100 ms) when concentrations of the precipitating solutions are increased to allow detection.[27] We saw in Fig. 6(d) that the HPC EF gave platelets rather than rods, suggesting that the HPC adsorbs on a different face to the methyl-group-dominated MC25 and the HPMCs. This would then modify the aggregation kinetics in a different crystallographic direction, *i.e.* modifying the ε–ε face aggregation and α–α face aggregation rates, as discussed in more detail below for the case of precipitation in the presence of acetate ions, where platelet particles were also observed.

Modifying copper oxalate morphology by using acetate ions

For the cobalt oxalate PMMA system the interaction seemed to be *via* a specific complexing interaction with the carboxylate functional group and the cobalt ion. Also, for the copper oxalate cellulose derivatives the adsorption seems to be driven by specific interactions with methyl and propyl cellulose derivatives giving elongated rods and platelet morphologies, respectively. To see if specific complexing species can influence the precipitation of copper oxalate we have investigated the addition of the acetate group to the precipitation system. Speciation diagrams to follow the effect of the acetate on the solution composition were calculated using a previously developed thermodynamic model for copper oxalate.[17]

In Fig. 7 two graphs are presented showing the copper species distribution as a function of the pH in the system $Cu(OH)_2$–$H_2C_2O_4$–HAc–[HNO_3/NaOH]–H_2O at 30 °C. Without acetate, with the ionic strength $\mu = 0.0202$ mol L^{-1} and the pH is 5.0, the solubility of copper oxalate equals 2.22×10^{-4} mol L^{-1}. As shown in Fig. 7(a), copper is mainly in solution in the form of the $[CuC_2O_4]^0$ complex (57%), followed by Cu^{2+} (26%) and by the $[Cu(C_2O_4)_2]^{2-}$ complex (18%). In the presence of 2×10^{-2} mol L^{-1} of sodium acetate (Fig. 7(b)), the $[CuC_2O_4]^0$ complex is still the major species but now only represents 42% of the total copper species. The $[Cu(C_2O_4)_2]^{2-}$ complex reaches

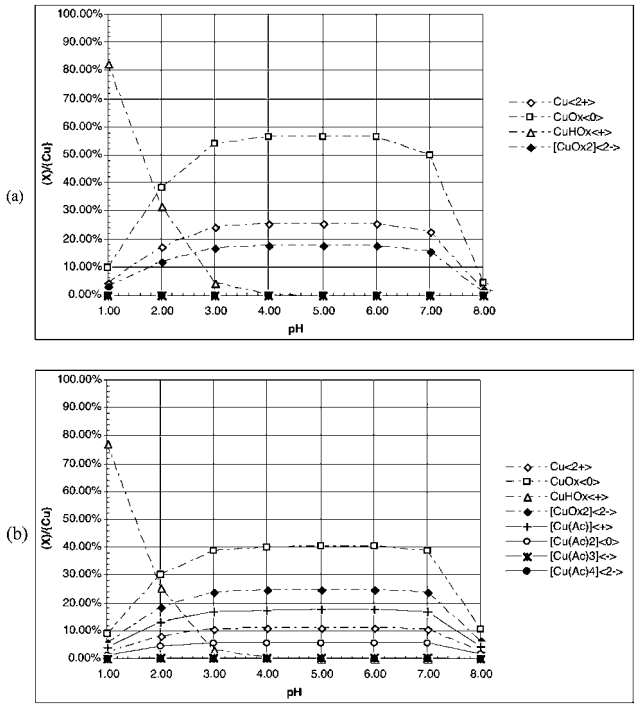

Fig. 7 Distribution of copper containing species as a function of pH in the system (a) without acetate $Cu(OH)_2$–$H_2C_2O_4$–[HNO_3/NaOH]–H_2O at 30 °C with $\mu = 0.0202$ mol L^{-1}, $(Ox^{2-}) = 9.08 \times 10^{-6}$ mol L^{-1}, {Cu} = {Ox} = 2.22×10^{-4} mol L^{-1}; (b) with acetate $Cu(OH)_2$–$H_2C_2O_4$–HAc–[HNO_3/NaOH]–H_2O at 30 °C with $\mu = 0.0200$ mol L^{-1}, $(Ox^{2-}) = 1.61 \times 10^{-5}$ mol L^{-1}, {Cu} = {Ox} = 3.12×10^{-4} mol L^{-1}.

24% instead of 18% followed by the $[CuAc]^+$ complex (17%) and Cu^{2+} (10%).

Copper oxalate presents a cushion-like morphology with an axial ratio of 0.5 (Fig. 8(a)). When precipitated in the presence of acetate ions a more plate-like morphology (Fig. 8(b)) is obtained with axial ratios of about 0.15. Both samples were identified to be exclusively $CuC_2O_4 \cdot xH_2O$ ($0 < x < 1$) using X-ray diffraction. The mean crystallite size was calculated in the [110] and [001] directions for both samples, as described previously.[5] In the presence of acetate, the mean size L_{110} decreases by 30% while it increases by 30% in the [001] direction (Table 3). In fact, the crystallite shapes are very similar but the primary nanocrystals have a tabular shape without acetate and a rod-like shape with acetate. The crystallite shape with acetate is very close to the

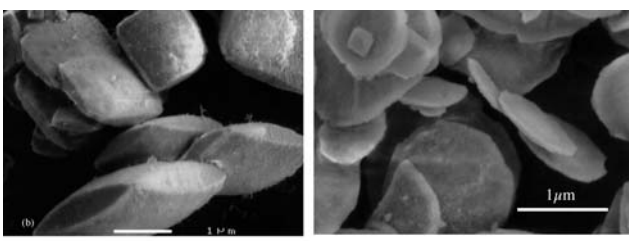

Fig. 8 Micrographs of (a) sample 1 prepared without additive showing a cushion-like morphology; (b) sample 2 prepared in the presence of acetate showing a plate-like morphology.

Table 3 Comparison of crystallographic cell parameters for copper oxalate powders precipitated: 1 without acetate ions; 2 with acetate ions. Mean crystallite sizes and total number of crystallites per sample are from X-ray diffraction data

	1	2
Cell parameter		
a/Å	5.3982 ± 0.0009	5.330 ± 0.001
b/Å	5.6075 ± 0.00087	5.660 ± 0.002
c/Å	2.5601 ± 0.00031	2.561 ± 0.0002
Mean crystallite size/nm		
L_{110}	69	43
L_{001}	49	78
Volume/μm^3	2.33×10^{-4}	1.44×10^{-4}
N_{cryst}/L^{-1} [a]	1.6×10^{15}	7.9×10^{14}

[a] Calculated from the total amount of precipitate in 1 L (1.3 g for sample 1 and 0.4 g for sample 2) and the copper oxalate density (3.5 g cm^{-3}).

crystallite shape of copper oxalate precipitated in the presence of 0.1563 g L^{-1} of HPMC,[4] but with a final particle shape which is an elongated rod rather than thin platelet.

One of the key factors in explaining the ordered aggregation of the crystallites and the increase of the axial ratio in the presence of HPMC is the anisotropy of the copper oxalate crystalline structure. The terminating surfaces of the crystallites are of two types ε (110 and $1\bar{1}0$ faces) and α (001 faces). These are expected to have different interfacial energies with respect to the surrounding solution. The ε surfaces are assumed to have a higher surface energy and interact preferentially with the HPMC to minimise the overall free energy.[5] The α type faces are more likely to have more polar terminations and have a lower interfacial energy. In the presence of the HPMC the ε faces lower their interfacial energy by adsorbing HPMC and the aggregation of the particles by α–α assembly is favoured leading to elongated particles along the 001 direction.[7]

The influence of the acetate ions on the crystallite shape changes the relative areas of the α and ε faces—increasing the proportion of ε- faces *i.e.* the higher energy surfaces. This makes ε–ε assembly the most favourable geometry both energetically and statistically (more likely during particle collisions) leading to the thin platelets (Fig. 8(b)). This assumption could not be verified from a crystallographic point of view using electron diffraction due to the decomposition of the thin copper oxalate particles under the electron beam. However, what has happened is the aggregation kinetics of our self-assembling crystallites has been modified and is linked to the change in the types of surfaces exposed to the solution. This can come about by the modifying the speed of growth along the different planes by changing the concentration of the species in solution and by specific adsorption of, for example, the acetate ion at the growing surface, changing its relative interfacial energy and growth rate. The lattice parameters reported in Table 3 show that the unit cell directions a and b change by about 1% (much more than the indicated standard deviation) after addition of acetate ions, whereas the c direction is almost unaffected. This result indicates that acetate ions can be adsorbed and incorporated in the oxalate particles. Adsorption/incorporation predominantly occurs on crystallographic surfaces perpendicular to the (001) plane and, consequently, the hypothesis that the surface energy of the ε faces

is modified by the acetate ions finds some support. The acetate ions also modify the solubility of the copper oxalate system which modifies the yield (reduced by 70%) and thus the number of crystallites per unit volume (calculated for yields with and without acetate—Table 3). The crystallite number density (number per unit volume) will also directly affect the aggregation rates. The number density is halved for precipitates prepared in the presence of acetate.

These results again indicate that the self-assembly of copper oxalate (and cobalt oxalate above) can be influenced by complexing molecules with respect to the metallic cation of the desired precipitate. The degree of adsorption and residence time of the adsorbed molecule on a particular crystal face can then influence either crystallite growth kinetics or aggregation kinetics. The next step towards a better control of the crystallite size and shape and the particle size, shape and nanostructure is through an atomistic understanding of these interactions in a dynamic system for example by using molecular dynamics simulations. The use of molecular dynamics simulations has recently helped elucidate key aspects of the adsorption conformation and residence time of polyacrylates and carboxylic acids at calcite surfaces.[28] To get more control and predictive power to allow us to produce nanostructured particles by design, atomistic molecular dynamic simulations in conjunction with the thermodynamic speciation and population balance modeling[29] offer great potential.

Conclusions

Two nanostructured oxalate systems have been investigated and a high degree of control of particle morphology can be provided using a different polymeric additives.

The cobalt oxalates in the presence of PMMA show a change in morphology from rods to platelets as the concentration of the PMMA in the precipitation system is increased. The crystallite sizes from XRD line broadening remained constant allowing us to conclude that the PMMA acted on the aggregation kinetics by adsorbing on specific surfaces. From electron diffraction we have shown that the growth along crystallographic direction [101] was significantly inhibited, indicating that the PMMA interacted specifically with the (101) faces.

Copper oxalates precipitated in the presence of different cellulose derived polymers with different molecular weights and functional groups (methyl and propyl) showed sensitivity to both molecular weight and functional group. Higher molecular weights did not influence the copper oxalate particle shape where cushion-like shapes were observed similar to precipitation without additives. This was interpreted as a kinetic effect. When using cellulose derivatives with only methyl groups on the cellulose elongated particles, similar to the HPMCs which had predominantly methyl substitutions (26% methyl and 4% propyl), were formed. With only propyl substituted celluloses platelet-like particles were observed suggesting interaction with different crystallite faces which in turn modified the aggregation or self-assembly stage of particle growth.

The presence of copper complexing ions, namely acetate ions in copper oxalate precipitation, modified significantly the morphology of the precipitated particles. The axial ratio was decreased from around 0.5 for cushion-like copper oxalate to 0.1–0.2 in the presence of the acetate ions. According to the solubility calculations, the key dissolved species involved in the precipitation is in both cases the neutral $[CuC_2O_4]^0$ complex. The mean crystallite volume was similar for both powders but the crystallite is more elongated along the [001] direction in the presence of acetate. The change in particle morphology is accounted for by changing the number and area of the hydrophobic and hydrophilic surfaces of the crystallite and is in agreement with other recent work on copper oxalate indicating that the self-assembly of these nanostructured particles depend greatly on the aggregation kinetics and thus the strength and residence times of polymeric additives or complexing moieties at the crystallite surface.

The atomistic modeling of the surface energies of the different faces of the copper and cobalt oxalates and the possible interaction of the polymers and acetate ions with specific surfaces using molecular dynamics is a key area for future development and substructure control of nanostructured particles.

Acknowledgements

The authors wish to thank Dr P. Moeckli and Dr Kurt Schenk for their help with the XRD study, Mr B. Senior for some of the SEM work and Dr J.-C. Valmalette for stimulating discussions.

The Swiss National Fund is gratefully acknowledged for its financial support. N. J. thanks the "Stiftung Entwicklungsfond Seltene Metalle" for a grant.

References

1 S. Mann, *Nature*, 1993, **365**, 499; H. Cölfen, and S. Mann, *Angew. Chem., Int. Ed.*, 2003, **42**, 2350–2365.
2 S. Mann and G. A. Ozin, *Nature*, 1996, **382**, 313.
3 S. Mann, J. M. Didymus, N. P. Sanderson, B. R. Heywood and E. J. A. Samper, *J. Chem. Soc., Faraday Trans.*, 1990, **86**, 1873.
4 A. S. Finnemore, M. R. J. Scherer, R. Langford, S. Mahajan, S. Ludwigs, F. C. Meldrum and U. Steiner, *Adv. Mater.*, 2009, **21**, 3928.
5 N. Jongen, P. BowenLemaître, J. Valmallette and H. J. Hofmann, *J. Colloid Interface Sci.*, 2000, **226**, 189; L. C. Soare, P. Bowen, J. Lemaitre and H. Hofmann, *J. Phys. Chem. B*, 2006, **110**, 17763.
6 O. Pujol, P. Bowen, P. A. Stadelmann and H. Hofmann, *J. Phys. Chem. B*, 2004, **108**, 13128.
7 J. Romann, V. Chevallier, A. Merlen and J.-C. Valmalette, *J. Phys. Chem. C*, 2009, **113**, 5068.
8 N. Jongen, H. Hofmann, P. Bowen and J. J. Lemaître, *J. Mater. Sci. Lett.*, 2000, **19**, 1073.
9 L. C. Soare, P. Bowen, J. Lemaître, H. Hofmann, M. Pijolat and F. Valdivieso, *Mater. Res. Soc. Symp. Proc.*, 2004, **788**, L1.4.1, Materials Research Society.
10 M. Paschoalino, N. C. Guedes, W. Jardim, E. Mielczarski, J. A. Mielczarski, P. Bowen and J. Kiwi, *J. Photochem. Photobiol., A*, 2008, **199**, 105–111.
11 J. Nyvlt, J. Ulrich *Admixtures in Crystallization*, 1995, VCH Publishers, New York, NY.
12 H. Coelfen, M. Antionetti, *Mesocrystals and Nonclassical Crystallization*, 2008, J. Wiley and Sons.
13 H. Yang, W. Yao, L. Yang, X. Maa, H. Wang, F. Yea and K. Wong, *J. Cryst. Growth*, 2009, **311**, 2682.
14 Z. Nan, X. Chen, Q. Yang and Z. Chen, *Mater. Res. Bull.*, 2010, **45**, 722.
15 E. Matijevic, *Chem. Mater.*, 1993, **5**, 412.
16 E. Matijevic, *Curr. Opin. Colloid Interface Sci.*, 1996, **1**, 176.
17 L. C. Soare, J. Lemaître, P. Bowen and H. Hofmann, *J. Cryst. Growth*, 2006, **289**(1), 278.

18 H. P. Klug; L. E. Alexander *X-Ray Diffraction Procedures for Polycrystalline and Amorphous Materials*, 1974, Wiley & Sons, New York, NY.
19 B. E. Warren, *Progress in Metal Physics*, 1959, **8**, 147.
20 G. Avond, H. Pezerat, J. Lagier and J. Dubernat, *Rev. Chim. Miner.*, 1969, **6**, 1095.
21 I. Sabbagh, M. Delsanti and P. Lesieur, *Eur. Phys. J. B*, 1999, **12**, 253.
22 I. Sabbagh and M. Delsanti, *Eur. Phys. J. E*, 2000, **1**, 75–86.
23 C. Ünaleroglu, B. Zümreoglu-Karan, S. Özcan and T. Firat, *J. Appl. Polym. Sci.*, 1995, **56**, 1239.
24 K. Veröhlen, H. Lewandowski, H.-D.- Narres and M. J. Schwuger, *Colloids Surf., A*, 2000, **163**, 45–63.
25 N. Jongen, M. Donnet, P. Bowen, J. Lemaitre, H. Hofmann, R. Schenk, C. Hofmann, M. Auon-Habbache, S. Guillemet-Fritsch, J. Sarrias, A. Rousset, M. Viviani, M. T. Buscaglia, V. Buscaglia, P. Nanni, A. Testino and Herguijuela, *Chem. Eng. Technol.*, 2003, **26**(3), 303–305.
26 U. Aschauer, J. Ebert, A. Aimable and P. Bowen, *Cryst. Growth Des.*, 2010, **10**(9), 3956–3963.
27 L. C. Soare, Ph.D Thesis EPFL no. 3083, Switzerland, 2004.
28 U. Aschauer, D. Spagnoli, S. C. Parker and P. Bowen, *J. Colloid Interface Sci.*, 2010, **346**, 226.
29 A. Testino, V. Buscaglia, M. T. Buscaglia, M. Viviani and P. Nanni, *Chem. Mater.*, 2005, **17**, 5346–5356.